

## 1. Introduction

X-Ray binaries with neutron star accretors are traditionally divided into two groups based on the masses of the donor stars. One is low-mass X-ray binaries (LMXBs) with donor stars less massive than  $\sim 1.5M_{\odot}$ , the other is high-mass X-ray binaries (HMXBs) with donor masses exceeding  $\sim 10.0M_{\odot}$ . In LMXBs mass is exchanged through Roche-Lobe overflow (RLOF), while in HMXBs, the accretor is likely to be fed by the stellar wind-induced mass loss of the companion. Systems with donor masses between  $1.5$  and  $10.0M_{\odot}$  are called intermediate-mass X-ray binaries (IMXBs). Few IMXBs have been discovered in the Galaxy. The reason is that, on one hand, mass transfer via RLOF is thought to be rapid and unstable due to the large mass ratio, leading to the formation of a common envelope; on the other hand, the donor stars at this mass range are unable to generate strong winds to power bright X-ray emission from the neutron star (van den Heuvel 1975).

Recent investigations on IMXB evolution lead to important realization on the stability of super-Eddington mass transfer, and suggest that many, or perhaps most, of the current LMXBs descended from IMXBs. The studies on the evolution of the LMXB Cyg X-2 (King & Ritter 1999; Podsiadlowski & Rappaport 2000; Kolb et al. 2000) indicate that the mass of the donor star in this system must have been substantially larger ( $\sim 3.5M_{\odot}$ ) than its current value ( $\sim 0.6M_{\odot}$ ), implying that intermediate-mass systems can survive the high mass transfer phase by ejecting most of the transferred mass. The calculations by Tauris, van den Heuvel, & Savonije (2000) have shown that the evolution of some IMXBs may survive a spiral-in and experience a highly super-Eddington mass transfer phase on a (sub)thermal timescale if the convective envelope of the donor star is not too deep. These systems provide a new formation channel for binary millisecond pulsars with heavy CO white dwarfs and relatively short orbital periods (3–50 days). Davies & Hansen (1998) have independently suggested that IMXBs may be the progenitors of recycled pulsars in globular clusters. These works emphasize the necessity of accurately defining an evolutionary path of IMXBs, and motivate systematic analysis of binary systems undergoing thermal timescale mass transfer.

Since the donor star in an IMXB is more massive than the accretor, the RL radius of the donor will shrink during the mass transfer. At the same time the donor star will either grow or shrink due to mass loss. The stability of the mass transfer depends on the radius-mass exponents for the donor and its RL (Soberman, Phinney, & van den Heuvel 1997),  $\xi_2 = (\partial \ln R_2 / \partial \ln M_2)$  and  $\xi_L = (\partial \ln R_L / \partial \ln M_2)_L$ , where  $\xi_2$  is the adiabatic or thermal response of the donor star to mass loss ( $M_2$  and  $R_2$  are the mass and radius of the donor star,  $R_L$  is its Roche-lobe radius, respectively). In general  $R_L$  decreases ( $\xi_L > 0$ ) when material is transferred from a relatively heavy donor to a light accretor, and vice versa. Donor stars with radiative envelopes will usually shrink ( $\xi_2 > 0$ ) in response to mass loss, while donor stars with a deep convective envelope expand rapidly ( $\xi_2 < 0$ ) in response to mass loss. The relative sizes of these parameters determine whether the mass transfer proceeds on either dynamical or thermal timescale. If  $\xi_2 > \xi_L$  the mass transfer is dynamically stable, occurring on either nuclear or thermal timescale. If  $\xi_2 < \xi_L$  the Roche lobe radius shrinks more rapidly than the adiabatic radius, and the mass transfer proceeds

on dynamical timescale which leads to a common envelope and a spiral in phase. The final product could be either a Thorn-Żytkow object or a short-period binary if the envelope is ejected (e.g. Tauris, van den Heuvel, & Savonije 2000; Podsiadlowski et al. 2002).

Podsiadlowski et al. (2002) made a survey of the X-ray binary sequences with the donor masses ranging from 0.6 to  $7M_{\odot}$ . These authors found the actual mass transfer rates through RLOF sometimes deviate from the values given by the traditional formula for thermal mass transfer<sup>1</sup>,

$$\dot{M}_{\text{th}} \simeq \frac{(M_2^i - M_1^i)}{\tau_{\text{KH}}}, \quad (1)$$

where  $M_1^i$  and  $M_2^i$  are the initial masses of the accretor and the donor respectively, and  $\tau_{\text{KH}}$  is the Kelvin-Helmholtz time scale

$$\tau_{\text{KH}} \simeq \frac{GM_2^2}{2R_2L_2}, \quad (2)$$

where  $G$  is the gravitational constant, and  $L_2$  the luminosity of the donor star. The work done by Langer et al. (2000) on the evolution of white dwarf binaries also indicates that Eq. (1) could overestimate the mean mass transfer rates by a factor of a few.

However, due to its simplicity, Eq. (1) has been widely used in population synthesis investigations (e.g. Hurley et al. 2002; Belczynski et al. 2007) for thermal timescale mass transfer in close binaries. The aim of this paper is to present a modified empirical formula to estimate the mean thermal timescale mass transfer rates onto neutron stars, by calculating the evolutions of IMXBs systematically. The results may be helpful to future investigations involving mass transfer processes in IMXBs. We describe the stellar evolution code and the binary model used in this study in §2. The calculated results and fitting formulae for the mass transfer rates are presented in §3. We conclude in §4.

## 2. Binary calculations

We have followed the evolution of the binary systems containing a neutron star and an intermediate-mass secondary star using an updated version of the evolution code developed by Eggleton (1971, see also Pols et al. 1995). The opacities in the code are from Rogers & Iglesias (1992) and from Alexander & Ferguson (1994) for temperatures below  $10^{3.8}$  K. We assume a mixing length parameter of  $\alpha = 2$ , and set the convective overshooting parameter to be 0.2. The metallicity of the secondary is taken to be  $Z = 0.02$  and 0.001, and the corresponding Helium abundance is 0.28 and 0.242, respectively. Each system is set to start with a neutron star of mass  $M_1 = 1.4M_{\odot}$  and a secondary of mass  $M_2$  from 1.6 to  $4.0M_{\odot}$ . Systems with donor mass higher than  $\sim 4.0M_{\odot}$  always experience unstable dynamical mass transfer (Tauris, van den Heuvel, & Savonije 2000; Podsiadlowski et al. 2002). The effective RL radius of the secondary is calculated with Eggleton's equation (Eggleton 1983),

$$\frac{R_L}{a} = \frac{0.49q^{2/3}}{0.6q^{2/3} + \ln(1 + q^{1/3})}, \quad (3)$$

<sup>1</sup> In Rapport, Di Stefano, & Smith (1994) the thermal timescale mass transfer rate is taken to be half of that given by Eq. (1).

where  $a$  is the orbital separation, and  $q = M_2/M_1$  is the mass ratio. We use the following formula to calculate the mass transfer rate from the donor star via RLOF (Eggleton 1971)

$$\dot{M}_2 = -RMT(R_2 - R_L)^3, \quad (4)$$

where  $RMT$  is a parameter adjusted automatically in the code, usually taken to be 500. The mass loss of the secondary via stellar wind is calculated according to the empirical formula given by Nieuwenhuijzen & de Jager (1990),

$$\log(-\dot{M}_{2w}) = -14.02 + 1.24 \log\left(\frac{L_2}{L_\odot}\right) + 0.16 \log\left(\frac{M_2}{M_\odot}\right) + 0.81 \log\left(\frac{R_2}{R_\odot}\right). \quad (5)$$

To follow the details of the mass transfer processes, we also include losses of orbital angular momentum due to mass loss, magnetic braking, and gravitational-wave radiation, although the last process is not important in this analysis. For magnetic braking, we use the standard angular momentum prescription suggested by Rapport, Verbunt, & Joss (1983). The Eddington luminosity of the neutron star is  $L_{\text{Edd}} = 4\pi GM_1 m_p / \sigma_T \simeq 1.3 \times 10^{38} (M_1/M_\odot)$  ergs $^{-1}$ , where  $m_p$  and  $\sigma_T$  are proton mass and the cross section of Thompson scattering, respectively. We limit the maximum accretion rate of the neutron star to the Eddington accretion rate  $\dot{M}_{\text{Edd}} = R_1 L_{\text{Edd}} / GM_1$  ( $\sim 1.5 \times 10^{-8} M_\odot \text{yr}^{-1}$  for a  $1.4 M_\odot$  neutron star), i.e.,  $\dot{M}_1 = -f \dot{M}_2$ , where

$$f = \begin{cases} 1 & \text{if } -\dot{M}_2 < \dot{M}_{\text{Edd}} \\ -\dot{M}_{\text{Edd}}/\dot{M}_2 & \text{if } -\dot{M}_2 \geq \dot{M}_{\text{Edd}} \end{cases}. \quad (6)$$

We let the excess mass be lost from the system with the specific orbital angular momentum of the neutron star. The orbital separation then changes according to the following equation (e.g. Soberman, Phinney, & van den Heuvel 1997)

$$\frac{\dot{a}}{a} = \frac{2\dot{J}}{J} - \frac{2\dot{M}_2}{M_2} - \frac{2\dot{M}_1}{M_1} + \frac{\dot{M}}{M} = \frac{2\dot{J}_{\text{MB}}}{J} - \frac{2\dot{M}_2}{M_2} \left[ (1-q) + \frac{q(1-f)}{2(1+q)} \right] \quad (7)$$

where  $M = M_1 + M_2$  is the total mass,  $J$  the orbital angular momentum, and  $\dot{J}_{\text{MB}}$  the rate of orbital angular momentum loss by magnetic braking.

### 3. Results

We have calculated a large number evolutionary sequences for IMXBs with various initial donor mass and orbital period, so that mass transfer starts when the donor star is on early and late main sequence (cases a1 and a2), in the Hertzsprung gap (cases b1, b2, b3) and on the giant branch (cases c1, c2 and c3), respectively. In Fig. 1 we show the initial distribution of the binaries in the  $M_2$  vs.  $\log a$  diagram. Triangles, squares, and diamonds in the figure correspond to the donor stars being main-sequence stars, subgiants, and red giants at the onset of mass transfer, respectively. We stop the calculation when either the mass transfer becomes dynamically unstable or dominated by the nuclear evolution of the donor. Obviously the occurrence of thermal timescale mass transfer depends on the initial mass ratio and the orbital period. When  $Z = 0.02$  we find that steady case a1 to case b2 thermal timescale mass transfer is possible if the initial donor mass is between  $1.6$  and  $3.6 M_\odot$ , while systems either containing a more massive donor or in cases b3 and c3 are subject to delayed unstable dynamical mass transfer. When  $Z = 0.001$  the calculated results

show that systems with donors between  $1.8$  and  $3.6M_{\odot}$  experience stable thermal timescale mass transfer in cases a1 to c2, otherwise the mass transfer is dynamically unstable.

Typical examples of the evolutionary sequences with  $Z = 0.02$  and  $0.001$  are shown in Figs. 2 and 3 respectively. In Fig. 2 the system contains a neutron star and a companion with initial mass of  $3.0M_{\odot}$ , which starts filling its RL roughly at the end of its central hydrogen burning. In Fig. 3 the donor has an initial mass of  $3.6M_{\odot}$  and starts filling its RL right after its helium ignition. In the figures we demonstrate the evolution of the mass transfer rate, the orbital period, the donor mass, and the neutron star mass with time. In Fig. 2 the mass transfer rate first rises rapidly to  $\sim 10^{-5.5} M_{\odot}\text{yr}^{-1}$ , then declines to a few  $10^{-8} M_{\odot}\text{yr}^{-1}$  after  $\sim 9$  Myr, and stays around this value for  $\sim 1$  Myr. During the former rapid mass transfer phase, the donor mass decreases from  $3 M_{\odot}$  to  $< 1 M_{\odot}$ , but most of the mass is lost from the system, and efficient accretion by the neutron star occurs during the latter part of the mass transfer phase. The orbital period first decreases to around 1.2 day, and then increases to  $\sim 30$  day at the end of mass transfer. Mass transfer shown in Fig. 3 is more rapid due to the more massive and evolved donor star, lasting around 0.1 Myr. About  $2.6 M_{\odot}$  mass is transferred from the donor star during this phase, most of which is lost from the system, and the neutron star mass hardly changes.

In our work the initiation ( $t_i$ ) and termination time ( $t_f$ ) of the thermal timescale mass transfer is assumed to be once the mass transfer rate exceeds and declines to the Eddington limit of the neutron star. The mean mass transfer rate  $\dot{M}_{\text{mean}}$  is calculated from the following equation,

$$\dot{M}_{\text{mean}} = \frac{M_2^i - M_2^f}{t_f - t_i}, \quad (8)$$

where  $M_2^i$  and  $M_2^f$  are the donor mass at  $t = t_i$  and  $t_f$ , respectively (stellar wind mass loss is negligible). In Tables 1 and 2 we list the calculated values of  $t_i$ ,  $t_f$ ,  $M_2^i$ ,  $M_2^f$ ,  $\dot{M}_{\text{mean}}$  and the maximum mass transfer rates  $\dot{M}_{\text{max}}$  for evolutions with  $Z = 0.02$  and  $0.001$ , respectively. For comparison, we also list the expected values of  $\dot{M}_{\text{th}}$  calculated with Eq. (1). Figures 4 shows the calculated mean mass transfer rates as a function of  $(M_2^i - M_1^i)/\tau_{\text{KH}}$ . A linear fit can be obtained to be

$$\dot{M}_{\text{mean}} \simeq 0.28 \frac{(M_2^i - M_1^i)}{\tau_{\text{KH}}} \quad (9)$$

for  $Z = 0.02$ , and

$$\dot{M}_{\text{mean}} \simeq 0.24 \frac{(M_2^i - M_1^i)}{\tau_{\text{KH}}} \quad (10)$$

for  $Z = 0.001$ .

#### 4. Summary and discussion

Our numerical calculations show that there are stable super-Eddington thermal timescale mass transfer processes in IMXB systems with donor mass between  $1.6$  and  $3.6M_{\odot}$  in both  $Z = 0.02$  and  $Z = 0.001$  cases. We find that on average the traditional expression (Eq. [1]) overestimates the thermal timescale mass transfer rates by a factor of  $\sim 4$ .

The results are obviously subject to various uncertainties in treating the mass transfer processes in binary evolution. One of the issues is the mass and angular momentum

loss during mass transfer. We have used Eddington-limited accretion rate for neutron star accretion. Recent observations of quite a few binary millisecond radio pulsars constrain the pulsar masses to  $\sim 1.35 M_{\odot}$  (Bassa et al. 2006, and references therein), suggesting that almost all of the transferred mass may be lost rather accreted by the neutron star during the IMXB and LMXB phase. If the lost mass carries the specific orbital angular momentum of the neutron star, the orbital shrinking during thermal timescale mass transfer would be slower than we have calculated. This can be clearly seen from Eq. (7) by setting  $f = 0$ . The effect on mass transfer is most significant for those binaries with mass transfer rates being mildly super-Eddington. For example, we find that the mean mass transfer rate is decreased by a factor  $\sim 5$  if the donor mass is  $\sim 1.5 - 2.0 M_{\odot}$  and  $Z = 0.02$ . We note that in white dwarf binary evolution, it has also been realized that the strong mass loss from the accretor can stabilize the mass transfer even for a relatively high mass ratio, avoiding the formation of a common envelope (Hachisu, Kato, & Nomoto 1996; Li & van den Heuvel 1997; Langer et al. 2000). If, however, part of the lost mass forms a circumbinary disk rather leaves the system (Soberman, Phinney, & van den Heuvel 1997), the disk would extract orbital angular momentum from the binary by tidal torque, enhancing the mass transfer rates and leading to more rapid orbital shrink (Spruit & Taam 2001).

It should be also noted that, during the evolution of an IMXB the strong X-ray radiation by the accretor and the accretion disk could illuminate the donor star and cause expansion of the donor and strong stellar wind (Podsiadlowski 1991; Hameury et al. 1993; Phillips & Podsiadlowski 2002), which would also lead to a higher mass transfer rate and shorter duration of mass transfer. As there is not a generally accepted theory on the irradiation effect, we have not include it in our calculations.

*Acknowledgements.* We are grateful to the referee for helpful comments. This work was supported by the Natural Science Foundation of China under grant numbers 10573010 and 10221001.

## References

- Alexander, D. R., & Ferguson, J. W. 1994, ApJ, 437, 879  
 Bassa, C. G., van Kerckwijk, M. H., Koester, D., & Verbunt, F. 2006, A&A, 456, 295  
 Belczynski, K. et al. 2007, accepted to ApJS (astro-ph/0511811)  
 Davies, M. B., & Hansen, B. M. S. 1998, MNRAS, 301, 15  
 Eggleton P. P., 1971, MNRAS, 151, 351  
 Eggleton, P. P. 1983, ApJ, 268, 368  
 Hachisu, I., Kato, M., & Nomoto, K. 1996, ApJ, 470, L97  
 Hameury, J.-M., King, A.R., Lasota, J.-P., & Raison, F., 1993, A&A, 277, 81  
 Hurley, J. R., Tout, C. A., & Pols, O. R. 2002, MNRAS, 329, 897  
 King, A. R. & Ritter, H., 1999, MNRAS, 309, 253  
 Kolb, U., Davies, M. B., King, A. R., & Ritter, H. 2000, MNRAS, 17, 438  
 Langer N., Deuschmann A., Wellstein S., & Hoflich P. 2000, A&A, 362, 1046  
 Li, X.-D. & van den Heuvel, E. P. J. 1997, A&A, 322, L9  
 Nieuwenhuijzen, H. & de Jager, C. 1990, A&A, 231, 134  
 Phillips, S. N., & Podsiadlowski, P. 2002, MNRAS, 337, 431  
 Podsiadlowski, P., 1991, Nature, 350, 136  
 Podsiadlowski, Ph., & Rappaport, S. 2000, ApJ, 529, 946

- Podsiadlowski, P., Rappaport, S., & Pfahl, E., 2002, *ApJ*, 565, 1107
- Pols, O., Tout, C. A., Eggleton, P. P., & Han, Z. 1995, *MNRAS*, 274, 964
- Rappaport, S., Di Stefano, R., & Smith, M. 1994, *ApJ*, 426, 692
- Rappaport, S. A., Verbunt, F., & Joss, P. C. 1983, *ApJ*, 275, 713
- Rogers, F. J. & Iglesias, C. A. 1992, *ApJS*, 79, 507
- Soberman, G. E., Phinney, E. S., & van den Heuvel, E. P. J., 1997, *A&A*, 327, 620
- Spruit, H. C. & Taam, R. E., 2001, *ApJ*, 548, 900
- Tauris, T., van den Heuvel, E. P. J., & Savonije, G. J. 2000, *ApJ*, 530, L93
- van den Heuvel, E. P. J. 1975, *ApJ*, 198, L109

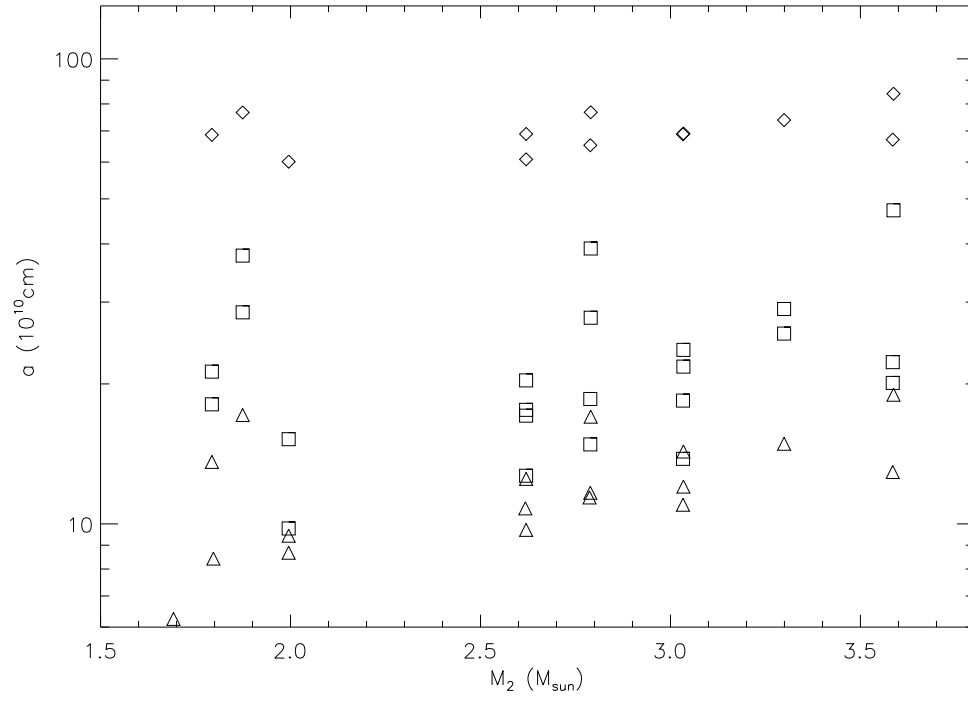


**Fig. 1.** The initial distribution of donor mass and orbital separation at the onset of mass transfer. The triangles, squares and diamonds refer to donors on main sequence, subgiant branch and red giant branch, respectively.

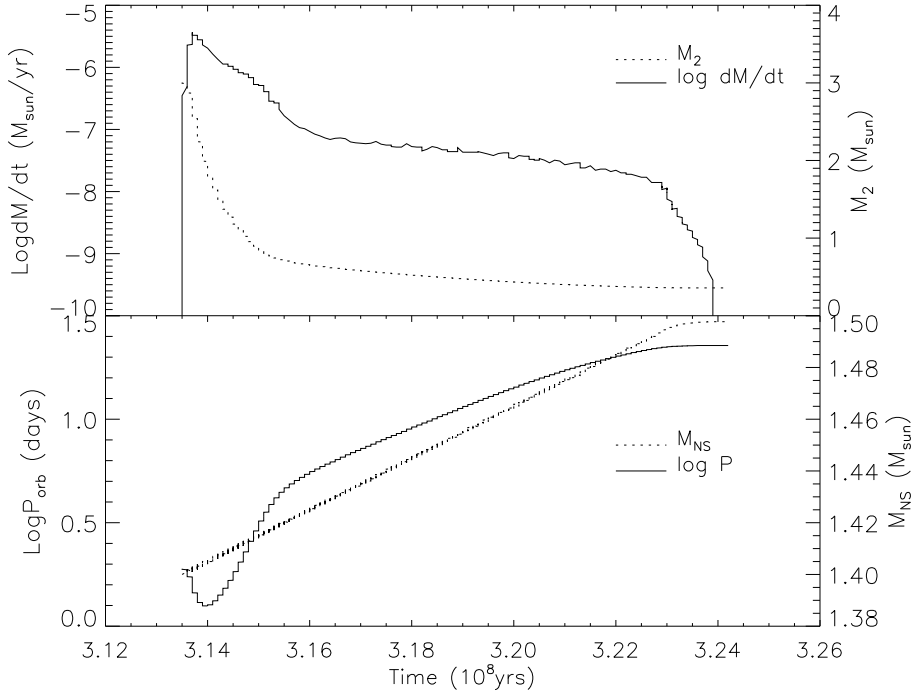


**Fig. 2.** The evolution of an IMXB with the donor of mass  $3.0M_{\odot}$  and  $Z = 0.02$ . The mass transfer starts right after the depletion of its core hydrogen. The solid and dotted lines show the evolution of the mass transfer rate and the donor mass in the upper panel, and the evolution of the orbital period and the neutron star mass in the lower panel, respectively.

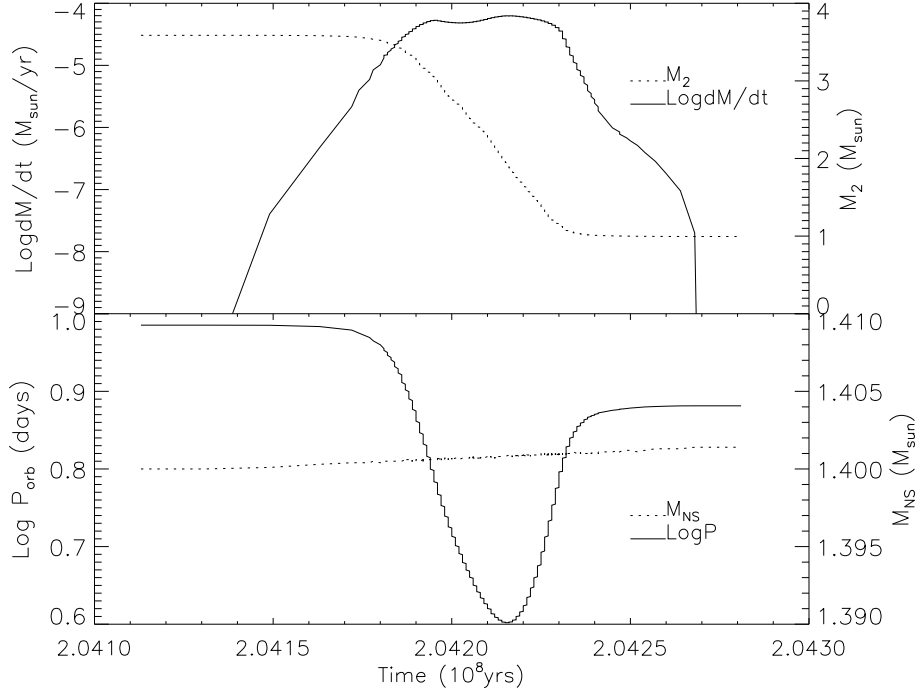


**Fig. 3.** Similar as Fig1. The evolution of an IMXB with the donor of mass  $3.6M_{\odot}$  and  $Z = 0.001$ . The mass transfer starts right after its central helium ignition . The solid and dotted lines show the evolution of the mass transfer rate and the donor mass in the upper panel, and the evolution of the orbital period and the neutron star mass in the lower panel, respectively.

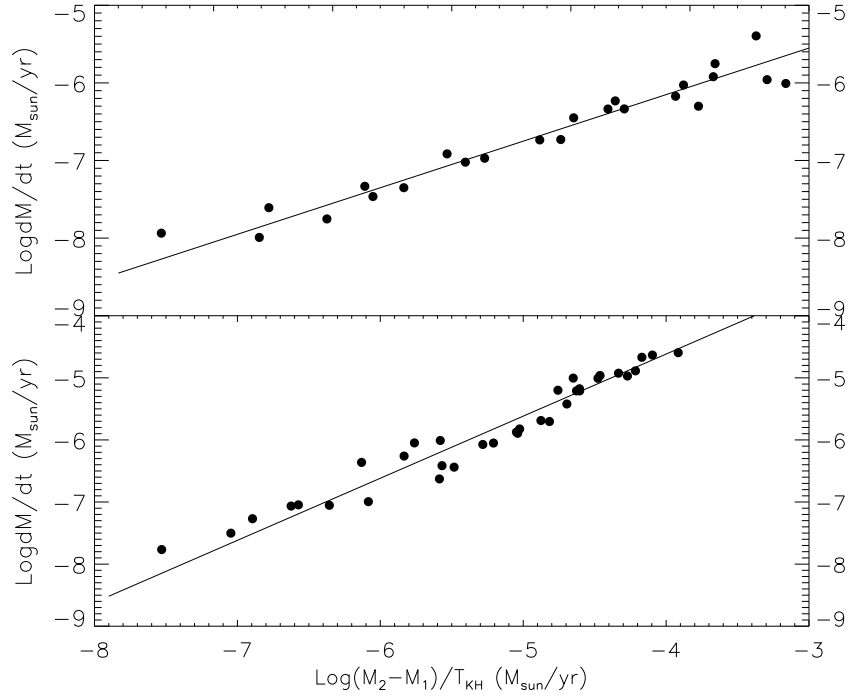


**Fig. 4.** The upper and lower panels show the fitting results for the mean thermal timescale mass transfer rates in  $Z = 0.02$  and  $Z = 0.001$  systems, respectively. The filled dots indicate the calculated results in this work.

**Table 1.** The calculated data of 24 evolutionary sequences with stable thermal timescale mass transfer ( $Z = 0.2$ ).  $\dot{M}_{\text{mean}}$ ,  $\dot{M}_{\text{max}}$  and  $\dot{M}_{\text{th}}$  are the mean mass transfer rates, the maximum mass transfer rates and the mass transfer rates calculated from Eq. (1), respectively.

$M_2$ ( $M_\odot$ )	Case	$t_i$ ( $10^8$ yr)	$M_2^i$ ( $M_\odot$ )	$t_f$ ( $10^8$ yr)	$M_2^f$ ( $M_\odot$ )	$\log \dot{M}_{\text{mean}}$ ( $M_\odot \text{yr}^{-1}$ )	$\log \dot{M}_{\text{max}}$ ( $M_\odot \text{yr}^{-1}$ )	$\log \dot{M}_{\text{th}}$ ( $M_\odot \text{yr}^{-1}$ )
1.6	a1	7.52	1.58	7.58	1.51	-7.94	-7.90	-7.72
1.8	a1	4.99	1.80	5.05	1.63	-7.61	-7.55	-7.27
2.0	a1	5.10	2.00	5.18	1.61	-7.33	-7.14	-6.87
2.3	a1	3.51	2.30	3.57	1.52	-6.91	-6.54	-6.52
3.0	a1	1.56	3.00	1.61	1.26	-6.45	-5.70	-5.99
3.3	a1	1.21	3.30	1.25	1.13	-6.23	-5.48	-5.81
1.8	a2	11.0	1.80	11.1	1.64	-7.75	-7.58	-7.02
2.0	a2	8.06	2.00	8.15	1.60	-7.35	-6.97	-6.70
2.3	a2	5.31	2.30	5.39	1.50	-6.97	-6.41	-6.36
2.6	a2	4.09	2.61	4.16	1.36	-6.73	-5.99	-6.04
3.0	a2	2.68	3.00	2.73	1.02	-6.34	-5.56	-5.78
3.3	a2	2.19	3.30	2.23	0.95	-6.17	-5.35	-5.56
3.6	a2	1.73	3.60	1.76	0.84	-5.92	-4.92	-5.40
1.6	b1	18.8	1.57	18.8	1.52	-7.99	-7.96	-7.31
1.8	b1	13.2	1.80	13.2	1.59	-7.46	-7.29	-6.83
2.0	b1	9.67	2.00	9.72	1.52	-7.02	-6.68	-6.44
2.3	b1	6.46	2.30	6.51	1.36	-6.7	-6.20	-6.13
2.6	b1	4.61	2.60	4.64	1.03	-6.34	-5.83	-5.84
3.0	b1	3.14	3.00	3.16	0.66	-6.03	-5.44	-5.53
3.3	b1	2.42	3.30	2.43	0.65	-5.75	-5.22	-5.39
3.6	b1	1.92	3.60	1.92	0.78	-5.39	-4.91	-5.22
3.0	b2	3.17	3.00	3.22	0.40	-6.30	-5.44	-5.46
3.3	b2	2.47	3.30	2.49	0.44	-5.96	-4.98	-5.18
3.6	b2	1.95	3.60	1.98	0.46	-6.00	-4.96	-5.10

**Table 2.** The calculated data of 34 evolutionary sequences with stable thermal timescale mass transfer ( $Z = 0.001$ ).

$M_2$ ( $M_\odot$ )	Case	$t_i$ ( $10^8$ yr)	$M_2^i$ ( $M_\odot$ )	$t_f$ ( $10^8$ yr)	$M_2^f$ ( $M_\odot$ )	$\log \dot{M}_{\text{mean}}$ ( $M_\odot \text{yr}^{-1}$ )	$\log \dot{M}_{\text{max}}$ ( $M_\odot \text{yr}^{-1}$ )	$\log \dot{M}_{\text{th}}$ ( $M_\odot \text{yr}^{-1}$ )
1.8	a1	3.29	1.70	3.47	1.39	-7.77	-7.48	-7.53
1.8	a2	7.33	1.80	7.52	1.21	-7.50	-6.23	-7.05
1.8	b2	9.01	1.80	9.13	0.80	-7.05	-6.21	-6.36
2.0	a2	5.52	2.00	5.67	1.17	-7.27	-6.40	-6.89
2.0	b1	6.40	2.00	6.55	0.73	-7.05	-6.043	-6.57
2.0	b2	6.85	1.87	6.96	0.69	-6.99	-4.14	-6.08
2.3	c1	6.04	2.31	6.05	0.87	-5.69	-5.40	-4.88
2.3	c2	5.75	2.31	5.76	0.96	-5.82	-5.64	-5.03
2.3	c3	6.10	2.31	6.11	0.92	-5.70	-5.37	-4.81
2.6	a2	3.07	2.62	3.11	0.84	-6.36	-5.50	-6.13
2.6	b1	3.35	2.62	3.38	0.56	-6.05	-5.43	-5.76
2.6	b2	3.42	2.62	3.44	0.47	-6.01	-5.31	-5.58
2.6	c1	4.44	2.62	4.442	0.77	-5.21	-5.07	-4.61
2.6	c2	4.31	2.62	4.31	0.73	-5.20	-4.91	-4.76
2.6	c3	4.43	2.62	4.43	0.77	-5.21	-4.82	-4.63
2.8	a2	2.64	2.79	2.68	0.81	-6.26	-5.39	-5.83
2.8	b1	2.93	2.79	2.99	0.40	-6.41	-5.23	-5.57
2.8	b2	2.97	2.79	3.00	0.42	-6.07	-5.10	-5.28
2.8	c1	3.80	2.78	3.80	0.82	-5.01	-4.64	-4.48
2.8	c2	3.72	2.79	3.72	0.79	-5.18	-4.71	-4.61
2.8	c3	3.76	2.79	3.76	0.81	-5.00	-4.67	-4.65
3.0	a2	2.37	3.03	2.48	0.40	-6.63	-5.13	-5.59
3.0	b1	2.40	3.03	2.47	0.41	-6.44	-5.08	-5.48
3.0	b2	2.45	3.03	2.48	0.45	-6.05	-4.94	-5.21
3.0	c1	3.10	3.03	3.11	0.89	-4.97	-4.42	-4.27
3.0	c2	3.01	3.03	3.01	0.85	-4.96	-4.54	-4.46
3.0	c3	3.11	3.03	3.12	0.89	-4.67	-4.38	-4.17
3.3	b2	2.03	3.30	2.05	0.49	-5.87	-4.58	-5.05
3.3	c1	2.54	3.29	2.55	0.97	-4.63	-4.24	-4.10
3.3	c2	2.47	3.30	2.48	0.92	-4.93	-4.38	-4.33
3.6	b1	1.69	3.59	1.71	0.52	-5.89	-4.05	-5.04
3.6	b2	1.70	3.59	1.71	0.56	-5.42	-3.94	-4.70
3.6	c1	2.10	3.59	2.10	1.05	-4.60	-4.05	-3.92
3.6	c2	2.04	3.59	2.05	1.00	-4.89	-4.20	-4.22